DOI: 10.1002/chem.200700785

A Gd^{3+}-Based Magnetic Resonance Imaging Contrast Agent Sensitive to β-Galactosidase Activity Utilizing a Receptor-Induced Magnetization Enhancement (RIME) Phenomenon

Kenjiro Hanaoka,[a] Kazuya Kikuchi,[b] Takuya Terai,[a] Toru Komatsu,[a] and Tetsuo Nagano*[a]

Abstract: Magnetic resonance imaging (MRI) permits noninvasive three-dimensional imaging of opaque organisms. Gadolinium (Gd^{3+}) complexes have become important imaging tools as MRI contrast agents for MRI studies, though most of them are nonspecific and report solely on anatomy. Recently, MRI contrast agents have been reported whose ability to relax water protons is triggered or greatly enhanced by recognition of a particular biomolecule. This new class of MRI contrast agents could open up the possibility of reporting on the physiological state or metabolic activity deep within living specimens. One possible strategy for this purpose is to utilize the increase in the longitudinal water proton r_1 relaxivity that occurs upon slowing the molecular rotation of a small paramagnetic complex, a phenomenon which is known as receptor-induced magnetization enhancement (RIME), by either binding to a macromolecule or polymerization of the agent itself. Here we describe the design and synthesis of a novel β-galactosidase-activated MRI contrast agent, the Gd^{3+} complex **[Gd-5]**, by using the RIME approach. β-Galactosidase is commonly used as a marker gene to monitor gene expression. This newly synthesized compound exhibited a 57% increase in the r_1 relaxivity in phosphate-buffered saline (PBS) with 4.5% w/v human serum albumin (HSA) in the presence of β-galactosidase. Detailed investigations revealed that RIME is the dominant factor in this increase of the observed r_1 relaxivity, based on analysis of Gd^{3+} complexes **[Gd-5]** and **[Gd-8]**, which is generated from **[Gd-5]** by the activity of β-galactosidase, and spectroscopic analysis of their corresponding Tb^{3+} complexes, **[Tb-5]** and **[Tb-8]**.

Keywords: biosensors · gadolinium complexes · lanthanides · luminescence · magnetic resonance imaging

Introduction

Magnetic resonance imaging (MRI) is a noninvasive imaging technique that can provide images of intact, opaque organisms in three dimensions, even deep within a specimen, without photobleaching or light scattering which are often observed in light-based microscopy imaging experiments.[1] Therefore, MRI is useful not only in clinical medicine, but also in experimental research.[1,2] Nowadays, there is a considerable interest in MRI contrast agents, which can improve the resolution of MR images.[1,2] The MR images are based upon the NMR signal from water protons, and the signal intensity depends upon the water concentration and relaxation time (T_1 and T_2).[2] Paramagnetic ions like the gadolinium ion (Gd^{3+}), primarily shorten the T_1 (spin–lattice) relaxation time with high efficacy by rapid exchange of inner-sphere water molecules with bulk solvent.[3] Thus, Gd^{3+}-based MRI contrast agents increase tissue contrast by increasing water proton relaxation, and are widely used in clinical diagnostics.[4] In Gd^{3+}-based MRI contrast agents, chelation of Gd^{3+} is required for safety reasons: Dissociation of Gd^{3+} from a MRI contrast agent is undesirable, as both the free metal and unchelated ligands are generally more toxic than the complex itself.[2,4] Commonly used MRI

[a] Dr. K. Hanaoka, T. Terai, T. Komatsu, Prof. Dr. T. Nagano
Graduate School of Pharmaceutical Sciences
The University of Tokyo
7-3-1, Hongo, Bunkyo-ku, Tokyo 113-0033 (Japan)
Fax: (+81) 3-5841-4855
E-mail: tlong@mol.f.u-tokyo.ac.jp

[b] Prof. Dr. K. Kikuchi
Department of Materials and Life Sciences
Graduate School of Engineering, Osaka University
2-1 Yamada-oka, Suita City, Osaka 565-0871 (Japan)

Supporting information for this article is available on the WWW under http://www.chemeurj.org/ or from the author.

contrast agents are mainly extracellular agents with nonspecific biodistribution.[4,5] In contrast, it is also possible to develop Gd^{3+} complexes with various chemical properties by means of appropriate ligand design for Gd^{3+},[6] and, indeed, some bioactivated MRI contrast agents have been reported for monitoring enzyme activity, Ca^{2+}, pH, $p(O_2)$, Zn^{2+}, and so on.[7] These MRI contrast agents show a change in the water proton relaxation time (T_1 or T_2) in response to the presence of specific biomolecules. Recently, attempts have been made to utilize MR imaging techniques to detect gene expression, and the development of these methods would allow MR imaging of the expression of specific genes.[8] For example, β-galactosidase is a commonly used gene expression marker, that is, gene expression is monitored by introducing a marker gene, lacZ, to follow the regulation of a gene of interest because it can easily be assayed and is not normally expressed in most mammalian tissues or cells.[9] Meade and co-workers developed the bioactivated MRI contrast agent, EgadMe, which reports on β-galactosidase activity to image the expression of a transgene.[10] The mechanism of the T_1 relaxation time change between two distinct relaxation states, long and short, is as follows. The enzyme substrate, galactopyranose, which is linked to the ligand, blocks the one remaining open coordination site of the chelated Gd^{3+}, inhibiting access of water to the chelated Gd^{3+} ion. The contrast agent is switched on when β-galactosidase cleaves the galactopyranose from the Gd^{3+} complex and the chelated Gd^{3+} ion becomes accessible to water. This agent has been successfully used in vivo to monitor gene expression in *Xenopus laevis*.[10a] Thus, this MRI contrast agent showed a change in the longitudinal relaxation time (T_1) in the presence of β-galactosidase by modulating the access of water molecules to the chelated Gd^{3+} ion. In addition to above results, β-galactosidase-activated MRI contrast agents with a range of chemical properties are also needed for further biological studies, so the development of novel β-galactosidase-activated MRI contrast agents with a different design approach would be helpful for studies of biological phenomena by monitoring gene expression. One possible approach for the development of biomolecule-activated MRI contrast agents is the RIME (receptor-induced magnetization enhancement) approach.[11] The binding of a MRI contrast agent to a macromolecule substantially slows molecular rotation of the Gd^{3+} complex, resulting in an additional increase in the r_1 relaxivity through the rotational correlation time τ_R.[2] When the Gd^{3+} complex binds to a macromolecule, the τ_R increases from that of a small molecule to that of the protein, and the r_1 relaxivity increases. The slower the Gd^{3+} complex tumbles, the longer the τ_R, leading to faster relaxation rates and, hence, higher r_1 relaxivity. The τ_R for small Gd^{3+} complexes is usually in the picosecond range (typically 50–200 ps), whereas the τ_R for a macromolecule such as albumin is in the nanosecond range (about 50 ns).[6a] This phenomenon is known as RIME. RIME agents have been reported for alkaline phosphatase and for carboxypeptidase B (part of the thrombin-activatable fibrinolysis inhibitor family), which regulate noncovalent binding of the agents to human serum albumin (HSA).[12,13] Another agent permitted the detection of yeast transcription repressor protein (Gal80) as MR images by utilizing a specific peptide-protein binding event,[14] and the enzyme carbonic anhydrase was selectively targeted with a sulfonamide substituent.[15] Moreover, oligonucleotide sequences have also been detected with iron oxide nanoparticles derivatized with oligonucleotide.[16] Hybridization with oligonucleotide-derived particles resulted in changes mainly in the spin–spin relaxation time (T_2) of adjacent water protons. Efficient polymerization of Gd^{3+} complexes can also be used to directly image the activity of enzymes such as myeloperoxidase (MPO) and matrix metalloproteinase 2 (MMP-2).[17,18]

Here, we report the design and synthesis of a novel β-galactosidase-activated MRI contrast agent based on the RIME approach (Figure 1). Reaction with β-galactosidase

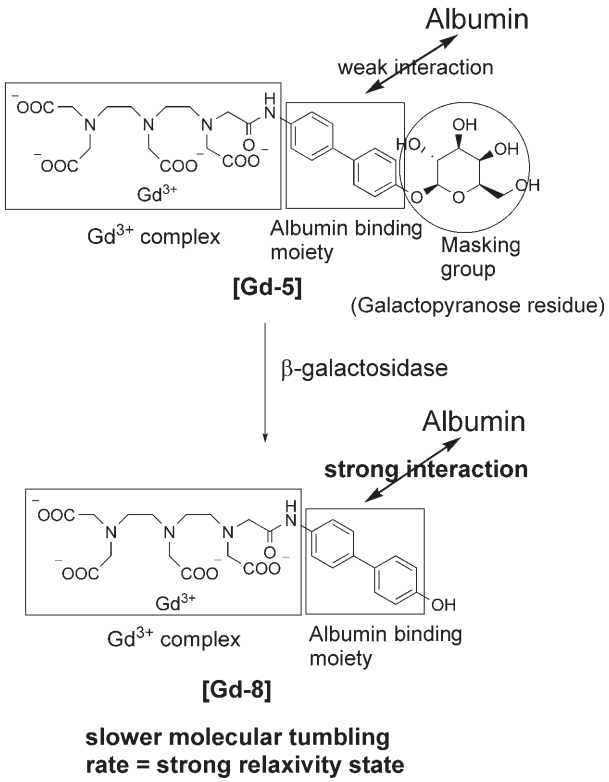

Figure 1. The RIME mechanism for the β-galactosidase-activated MRI contrast agent **[Gd-5]**. In **[Gd-5]**, a Gd^{3+} complex is coupled to an albumin binding moiety that is masked by the galactopyranose residue. The galactopyranose residue of **[Gd-5]** is designed to be cleaved by β-galactosidase, transforming **[Gd-5]** to **[Gd-8]**, and this cleavage promotes albumin binding of the Gd^{3+} complex.

yielded a 57% increase in the r_1 relaxivity in phosphate-buffered saline (PBS) with 4.5% w/v HSA. Cleavage of the galactopyranose moiety from the aryl group of the Gd^{3+} complex increases the hydrophobicity of the aryl group, thereby increasing the HSA binding affinity. The greater binding of the Gd^{3+} complex to the macromolecule, HSA, increases

the r_1 relaxivity. We also confirmed the mechanism of this increase in the r_1 relaxivity.

Results and Discussion

Design and synthesis of [Gd-5] and [Gd-8]: The Gd^{3+} complex, **[Gd-5]**, was designed to detect β-galactosidase activity through conversion of the MRI-silent agent into an activated MRI agent, **[Gd-8]** (Figure 1). The **[Gd-5]** is composed of three moieties: 1) a masking group consisting of galactopyranose; 2) an albumin-binding moiety, the biphenyl group; 3) an MRI signal-generating moiety, which is a Gd^{3+} complex. This design relies upon enzymatic transformation of a Gd^{3+} complex with poor albumin affinity and concomitant low relaxivity into one with high albumin affinity and high relaxivity. The biphenyl group was selected as the albumin binding group, because the biphenyl residue is known to possess high albumin binding affinity.[4,13,19] A substrate for β-galactosidase, galactopyranose, was used as a masking group, affording extremely high hydrophilicity compared with the hydrophobicity of the biphenyl group. Hydrolysis of the galactopyranose moiety unblocks the hydrophobicity of the biphenyl group, thereby increasing the albumin binding affinity. Thus, in **[Gd-5]**, a masking group that inhibits albumin binding was expected to be removed by the enzymatic activity, to expose an albumin-binding group with high affinity. The strong interaction of the Gd^{3+} complex with a macromolecule such as albumin increases the r_1 relaxivity owing to the RIME phenomenon. The synthetic schemes for the lanthanide complexes, **[Gd-5]** and **[Gd-8]**, and details of the chemical characterization of compounds are provided in the Supporting Information.

Longitudinal relaxation time T_1 measurements of [Gd-5] with β-galactosidase: The longitudinal relaxation times T_1 of **[Gd-5]** were measured in the presence of β-galactosidase or heat-inactivated β-galactosidase with 4.5% w/v HSA in phosphate-buffered saline (PBS; pH 7.4), at 20 MHz (0.47 T), at 37°C (Figure 2). The value of $1/T_1$ increased from 3.5 to 5.5 s^{-1} between 0 and 250 min in the presence of β-galactosidase (113 nM), whereas the value of $1/T_1$ changed only slightly from 3.8 to 4.0 s^{-1} between 0 and 250 min on exposure to heat-inactivated β-galactosidase (113 nM). We also assessed the ability of β-galactosidase to remove the galactopyranose masking group from **[Gd-5]** by high-pressure liquid chromatography (HPLC) analysis (Figure 3).

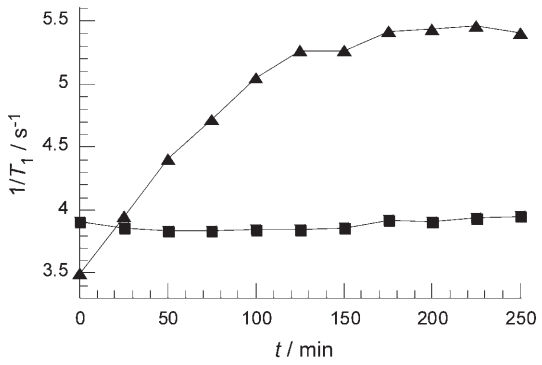

Figure 2. Time course of the β-galactosidase-induced (113 nM; ▲) and heat-inactivated β-galactosidase-induced (113 nM; ■) changes in the value of $1/T_1$ [s^{-1}], of 0.5 mM **[Gd-5]** solution at 20 MHz, 37°C in phosphate-buffered saline (PBS; pH 7.4) with 4.5% w/v human serum albumin (HSA).

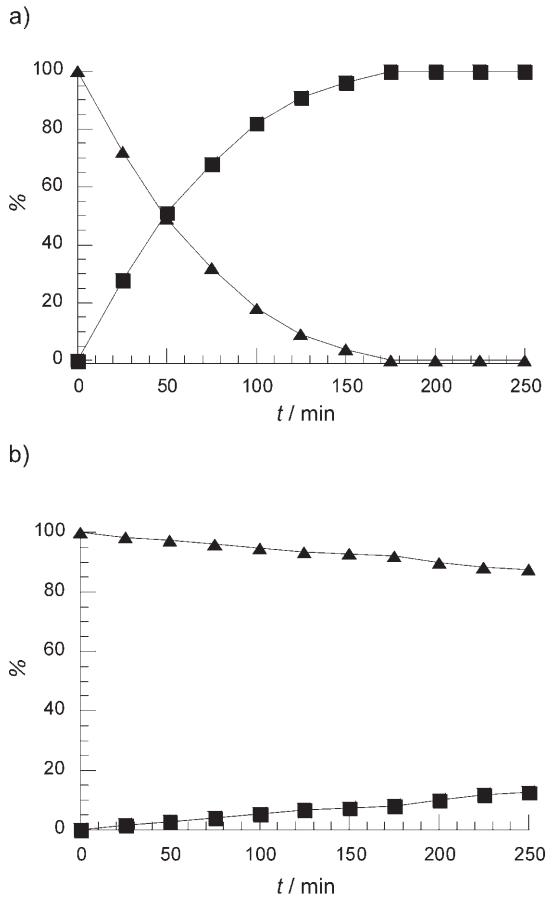

Figure 3. Time course of the conversion of **[Gd-5]** to **[Gd-8]**; the distribution of reaction species was quantified by HPLC analysis on the basis of the absorbance at 300 nm. The Gd^{3+} complex, **[Gd-5]** (0.5 mM) was incubated with: a) β-Galactosidase (113 nM) (**[Gd-5]**: ▲, **[Gd-8]**: ■) or; b) heat-inactivated β-galactosidase (113 nM) (**[Gd-5]**: ▲, **[Gd-8]**: ■) at pH 7.4, and 37°C, in phosphate-buffered saline (PBS) in the presence of 4.5% w/v human serum albumin (HSA).

This HPLC analysis showed that the Gd^{3+} complexes, **[Gd-5]** and **[Gd-8]**, had distinct retention times, and **[Gd-5]** was converted into **[Gd-8]** in the presence of β-galactosidase (113 nM), whereas essentially no change was observed upon the addition of heat-inactivated β-galactosidase (113 nM). The HPLC experiments confirmed the enzymatic processing of **[Gd-5]** by the β-galactosidase. Thus, **[Gd-5]** exhibited a β-galactosidase-induced RIME effect, accompanying the removal of the galactopyranose residue of **[Gd-5]**.

The r_1 relaxivity of Gd^{3+} complexes, [Gd-5] and [Gd-8]: The paramagnetic species, Gd^{3+}, acts as a catalyst to relax bulk water protons by fast exchange of the coordinated

water with bulk water (inner-sphere contribution). There is also a relaxation increase provided by the Gd^{3+} ion to water molecules which are diffusing close to the Gd^{3+} ion (second-sphere and outer-sphere contributions). The observed longitudinal relaxation rate $(1/T_1)_{obs}$ of the solvent water protons is known to depend on the concentration of Gd^{3+} ions according to Equation (1) :

$$(1/T_1)_{obs} = (1/T_1)_d + r_1[Gd] \quad (1)$$

where $(1/T_1)_{obs}$ is the observed relaxation rate of water protons in the presence of Gd^{3+}, and $(1/T_1)_d$ is the diamagnetic relaxation rate of water protons in the absence of Gd^{3+}. The longitudinal relaxivity value, r_1, refers to the amount of increase in $1/T_1\ s^{-1}$ per millimolar concentration of agent (given as mM^{-1} Gd), and [Gd] is the millimolar concentration of Gd^{3+} ions. Therefore, a plot of $(1/T_1)_{obs}$ versus Gd^{3+} concentration would give the r_1 relaxivity as the slope, and the r_1 relaxivity, normally expressed in units of $mM^{-1}\,sec^{-1}$, reflects the ability of a Gd^{3+} complex to increase relaxation. The water proton relaxivities, r_1, of **[Gd-5]** and **[Gd-8]** were determined at 20 MHz (0.47 T), at 25 or 37 °C, and are shown in Table 1. In the absence of HSA, the r_1 relaxivities

Table 1. The r_1 relaxivity [$mM^{-1}\ s^{-1}$] (20 MHz) in PBS with 4.5 % HSA or PBS.

Compound	HSA[a]		PBS[b]	
	25 °C	37 °C	25 °C	37 °C
[Gd-5]	6.34	6.06	5.80	5.35
[Gd-8]	8.76	9.51	4.11	3.87

[a] Human serum albumin (HSA) (4.5 % w/v) in phosphate-buffered saline (PBS; 137 mM NaCl, 8.10 mM Na_2HPO_4, 2.68 mM KCl, 1.47 mM KH_2PO_4, pH 7.4). [b] PBS only.

of **[Gd-5]** are higher than those of **[Gd-8]** at both 25 and 37 °C. However, in PBS with 4.5 % w/v HSA at 25 °C, the r_1 relaxivity of **[Gd-8]** is higher than that of **[Gd-5]** by 38 % as a consequence of a higher albumin binding affinity; at 37 °C, where the exchange of Gd^{3+}-bound water molecules is more facile, the r_1 relaxivity of **[Gd-8]** is higher than that of **[Gd-5]** by 57 %. From these results, it was considered that the increase of the $1/T_1$ value of **[Gd-5]** in Figure 2 was a consequence of enzymatic cleavage of the galactopyranose residue of **[Gd-5]** by the β-galactosidase activity. Moreover, the r_1 relaxivity of **[Gd-5]** at 20 MHz showed similar values in the absence and the presence of HSA, indicating that **[Gd-5]** hardly interacts with HSA.

Albumin binding study: We investigated the noncovalent interaction between **[Gd-5]** or **[Gd-8]**, and HSA. To demonstrate the extent of relaxation enhancement, the E-titration is shown in Figure 4.[2,11a] The longitudinal water proton relaxation times T_1 of a 0.1 mM solution of **[Gd-5]** or **[Gd-8]** in PBS with various concentrations of HSA (0–3.35 mM (0–22.5 % w/v)) were measured at 20 MHz (0.47 T), 37 °C. The results were expressed in terms of the enhancement factor ε^*, that is, the ratio of paramagnetic longitudinal relaxation

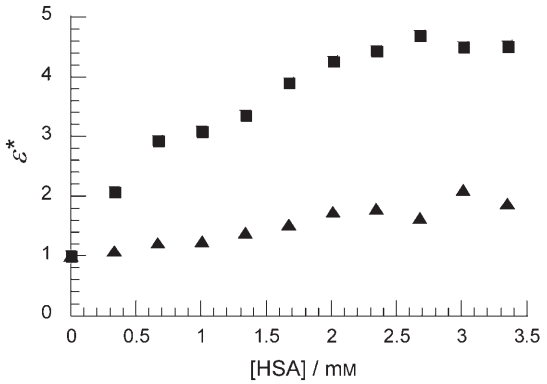

Figure 4. E-titration data for **[Gd-5]** and **[Gd-8]**. ε^* versus [human serum albumin (HSA)] in mM, at 37 °C, in phosphate-buffered saline (PBS, pH 7.4) at 20 MHz, 0.47 T. Each solution contains various concentrations of HSA (0–22.5 % w/v (=0–3.35 mM) with 0.1 mM **[Gd-5]** (▲) or **[Gd-8]** (■).

rates ($(1/T_1)_{para}$ [s^{-1}]) in the presence and the absence of HSA were plotted versus increasing HSA concentration at a constant concentration of **[Gd-5]** or **[Gd-8]** (0.1 mM) [Eq. (2)] :

$$\varepsilon^* = \frac{(1/T_1)^{Alb}_{obs} - (1/T_1)^{Alb}_{dia}}{(1/T_1)^{PBS}_{obs} - (1/T_1)^{PBS}_{dia}} = \frac{(1/T_1)^{Alb}_{para}}{(1/T_1)^{PBS}_{para}} \quad (2)$$

where the *obs*, *para*, and *dia* subscripts refer to the observed, paramagnetic, and diamagnetic species, respectively, and the *Alb* and *PBS* superscripts refer to "in PBS containing human serum albumin" and "in PBS", respectively. The longitudinal water proton relaxation times T_1 of aqueous solutions without Gd^{3+} complexes were measured as the diamagnetic contribution. The longitudinal relaxation rate ($1/T_1$ [s^{-1}]) increase of **[Gd-8]** solutions in the presence of HSA was much larger than that of **[Gd-5]** solutions, and did not increase linearly with the concentration of HSA, suggesting protein binding. There was a 1.9- or 4.5-fold increase in the enhancement factor ε^* upon binding to HSA for **[Gd-5]** or **[Gd-8]**, respectively. Small parts of these increases in ε^* can be ascribed to the misleading apparent amount of water molecules (ref. [4], p. 2342). For example, ≈3 mM HSA solution contains more than 20 % protein and hence less than 80 % water, because of the high molecular weight of HSA. The molar concentration of 1 mmol Gd^{3+} in a liter of 20 % w/v HSA is written as 1 mM, but the actual molar concentration would be 1.25 mM. However, the increase of ε^* for **[Gd-8]** is sufficiently large even when this problem is taken into consideration. Therefore, the enhancement factor ε^* for **[Gd-8]** suggests a high affinity of **[Gd-8]** for the albumin, whereas the slight increase of ε^* for **[Gd-5]** can be interpreted as indicating a weak interaction with the albumin.

Further, the binding interaction strengths of **[Gd-5]** and **[Gd-8]** to HSA were calculated by using the above E-titration experimental data.[2,11b,c,20] The observed longitudinal water proton relaxation rate, r_{1obs} [s^{-1}] is given by the sum of

three contributions, $r_{1p}{}^{F}$ [$mM^{-1}\,s^{-1}$], $r_{1p}{}^{B}$ [$mM^{-1}\,s^{-1}$], and r_{1dia} [s^{-1}]:

$$r_{1obs}-r_{1dia}=(r_{1P}{}^{F}[Gd]+r_{1p}{}^{B}[Gd\text{-}HSA])\times 1000 \quad (3)$$

where $r_{1p}{}^{F}$ and $r_{1p}{}^{B}$ are the r_1 relaxivity [$mM^{-1}\,s^{-1}$] of the Gd^{3+} complex and of the paramagnetic macromolecular, Gd^{3+} complex-HSA adduct, respectively, and r_{1dia} [s^{-1}], is the diamagnetic contribution of the observed longitudinal water proton relaxation rate r_{1obs} [s^{-1}], at 20 MHz, 37 °C. [Gd], in M, is the concentration of the Gd^{3+} complex, and [Gd-HSA], in M, is the concentration of the Gd^{3+} complex-HSA adduct. The determination of the binding parameter nK_A [M^{-1}] (K_A: association constant; n: number of independent binding sites on the protein) for the equilibrium :

$$Gd+HSA \underset{}{\overset{K_A}{\rightleftharpoons}} Gd{-}HSA \quad (4)$$

is possible through the following equations :

$$K_A=\frac{[Gd{-}HSA]}{[Gd]\cdot[n\cdot HSA]} \quad (5)$$

By combining Equations (3) and (5) we obtain Equation (6), which allows the nonlinear fitting of the experimental data :

$$r_{1obs}-r_{id}=\left(r^{F}\cdot B+(r^{B}-r^{F})\times\frac{K_AA+K_AB+1-\sqrt{(K_AA+K_AB+1)^2-4K_A{}^2AB}}{2K_A}\right)\times 1000 \quad (6)$$

where A and B [both in M], are the total molar concentrations of HSA and the Gd^{3+} complex, respectively. The fitting of the experimental data into Equation (6) provided an assessment of the binding strength, nK_A [M^{-1}], and the r_1 relaxivity [$mM^{-1}\,s^{-1}$], of the macromolecular adduct ($r_1{}^{B}$ [$mM^{-1}\,s^{-1}$]) (see the Supporting Information). The interaction strength of **[Gd-8]** with HSA was fairly strong ($nK_A=7.0\times10^{2}\,M^{-1}$) and the r_1 relaxivity of the paramagnetic macromolecular **[Gd-8]**-HSA adduct ($r_1{}^{B}$) was 20 $mM^{-1}\,s^{-1}$, at 20 MHz and 37 °C, whereas the interaction of **[Gd-5]** with HSA was rather weak ($nK_A<1.0\times10^{2}\,M^{-1}$).

Further, we examined whether various other species of albumins, such as, rat, bovine, and rabbit serum albumins, could serve as host macromolecules for **[Gd-8]**, like HSA. When **[Gd-5]** (0.1 mM) was incubated with β-galactosidase (1.13 μM), at 37 °C, for 30 min, in PBS, with 4.5 % w/v human, rat, bovine, or rabbit serum albumin, all solutions showed similar decreases of the longitudinal relaxation time (T_1) of water protons (see Supporting Information).

Time-resolved luminescence and UV/Vis absorption spectra of [Tb-5] and [Tb-8]: The chemical properties of **[Gd-5]** and **[Gd-8]** were further assessed by analyzing the luminescence and chemical properties of the terbium trivalent ion (Tb^{3+}) complexes of chelator **5** and **8**, **[Tb-5]** and **[Tb-8]** (Figure 5). Lanthanide complexes, in particular complexes of Tb^{3+} and Eu^{3+} (the europium trivalent ion), have advantageous spectroscopic characteristics, such as, long luminescence lifetimes of the order of milliseconds, narrow emission peaks, a large Stoke's shift of >150 nm, and excellent water solubility.[21] This extremely long luminescence lifetime of lanthanide ions allows a time-resolved detection procedure to be employed, because typical fluorescence lifetimes are in the nanosecond region; that is, a delay time is set between the excitation pulse and the measurement of the lanthanide luminescence, during which the background fluorescence and scattered light decay to negligible levels.[22] Therefore, time-resolved luminescence measurements offer a better signal-to-noise ratio, and the lanthanide luminescence has been exploited in a number of useful detection systems for time-resolved assays in the fields of medicine, biotechnology, and biological science.[23] We prepared **[Tb-5]** and **[Tb-8]** as homologues of **[Gd-5]** and **[Gd-8]**, because the Tb^{3+} ion possesses the same charge as Gd^{3+}, as well as similar ionic radius and coordination chemistry to the Gd^{3+} ion.[24] The synthetic schemes for **[Tb-5]** and **[Tb-8]** and details of the chemical characterization of compounds are provided in the Supporting Information. As regards the metal-based luminescence properties, 25 μM aqueous solutions of **[Tb-5]** and **[Tb-8]** (in 100 mM HEPES buffer; pH 7.4) were relatively brightly luminescent upon excitation at 254 nm with a TLC plate reader lamp, and these emissions of **[Tb-5]** and **[Tb-8]** were observed with the naked eye (see Supporting Information).

First, the UV/Vis absorption spectrum of **[Tb-5]** (50 μM) and **[Tb-8]** (50 μM) was measured in 100 mM HEPES buffer at pH 7.4, 25 °C. The absorption spectra of **[Tb-5]** and **[Tb-8]** were similar, that is, **[Tb-5]** showed a λ_{max} at 279 nm tailing out to 330 nm, and **[Tb-8]** showed a λ_{max} at 281 nm tailing to 330 nm (Figure 6a). These absorption spectra can be mainly ascribed to the biphenyl substituent, because the bands observed in Tb^{3+} absorption spectra are usually very weak, that is, molar absorption coefficients (ε) of lanthanide(III) ions are usually $<1\,dm^3\,mol^{-1}\,cm^{-1}$.[21] Second, the time-resolved luminescence spectrum of **[Tb-5]** (50 μM) or **[Tb-8]** (50 μM) was measured in 100 mM HEPES buffer (pH 7.4) upon excitation of the biphenyl substituent (excitation at 280 nm) for both **[Tb-5]** and **[Tb-8]**. The time-resolved luminescence spectra of **[Tb-5]** and **[Tb-8]**, with a delay time of 50 μs, displayed four bands (490, 545, 586, and 622 nm), arising from transitions from the emissive $^5D_4$ state to the ground-state manifolds, $^7F_6$, $^7F_5$, $^7F_4$, and $^7F_3$, respectively (Figure 6b).[21a,b] On the basis of the above spectroscopic results, the biphenyl substituent, which is the albumin-binding group, serves as a sensitizing chromophore for Tb^{3+} in the luminescent Tb^{3+} complexes, **[Tb-5]** and **[Tb-8]**.

The time-resolved luminescence spectra, with a delay time of 50 μsec, of **[Tb-5]** (50 μM) were measured in 100 mM HEPES buffer at pH 7.4, 25 °C excited at the absorbance maximum (λ_{max}) wavelength of the biphenyl group (280 nm) during the enzyme (β-galactosidase) reaction. Addition of β-

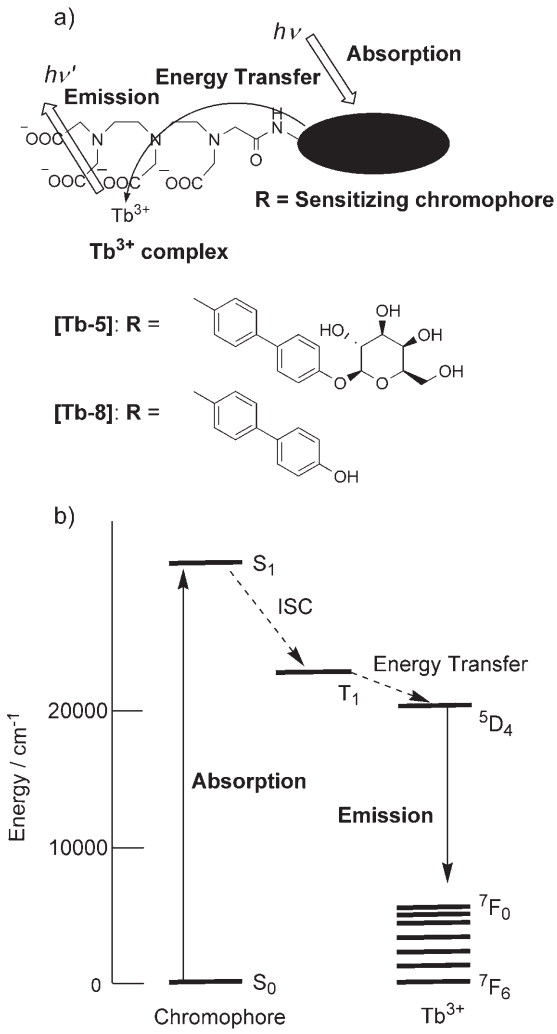

Figure 5. a) Structures of Tb^{3+} complexes, **[Tb-5]** and **[Tb-8]**, and schematic view of a chromophore incorporated into a terbium emitter. The emission from Tb^{3+} after excitation of the sensitizing chromophore on Tb^{3+} complexes, **[Tb-5]** and **[Tb-8]**, is shown. b) The general chromophore-to-terbium-ion sensitization process. Light absorption and lowest-lying singlet excited state (S_1) formation at the sensitizing chromophore are followed by intersystem crossing (ISC), resulting in population of the triplet excited state (T_1) of the sensitizing chromophore. Subsequent chromophore-to-Tb^{3+} energy transfer leads to a metal-centered emission, which is derived from transitions from Tb^{3+}-emitting states to the relevant ground states.

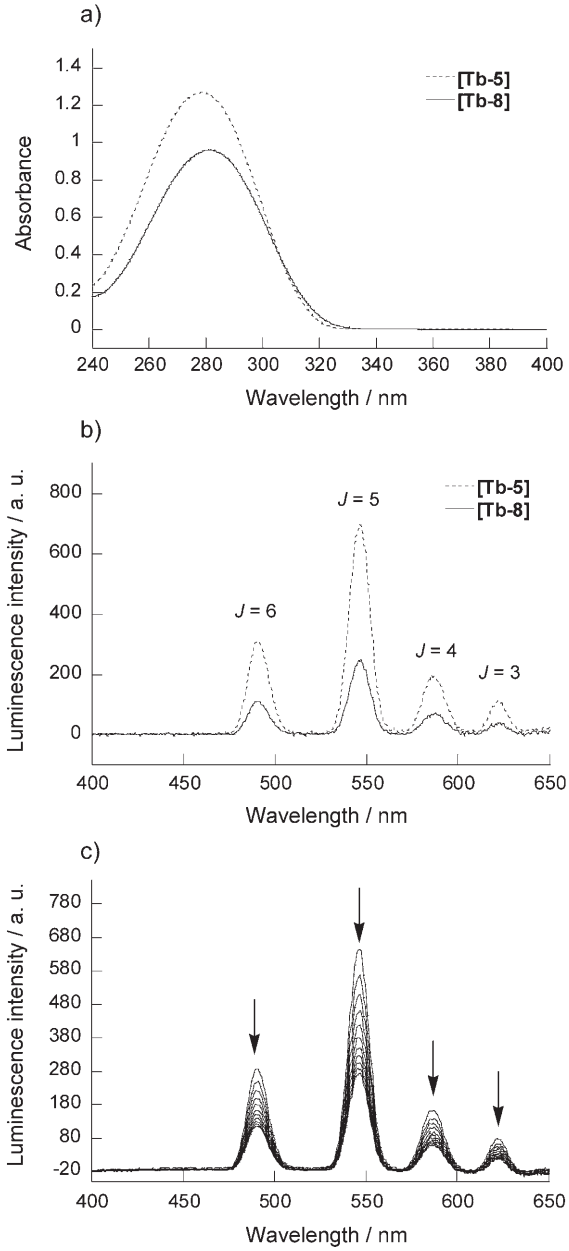

Figure 6. Spectroscopic characteristics of solutions of **[Tb-5]** and **[Tb-8]** upon addition of β-galactosidase. a) Absorbance spectra of 50 μM aqueous solution (100 mM HEPES buffer, pH 7.4) of **[Tb-5]** and **[Tb-8]** at 25 °C (**[Tb-5]**: – – –, **[Tb-8]**: ——). b) Time-resolved emission spectra (excitation at 280 nm) of **[Tb-5]** and **[Tb-8]** (50 μM) (**[Tb-5]**: – – –, **[Tb-8]**: ——). These spectra were measured in 100 mM HEPES buffer at pH 7.4 and 25 °C by using a delay time of 50 μs and a gate time of 1.00 ms. The bands arise from $^5D_4 \rightarrow {}^7F_J$ transitions; the J values of the bands are labeled. c) Time-resolved emission spectra (excitation at 280 nm) of **[Tb-5]** (50 μM) after the addition of β-galactosidase (113 nM) in 100 mM HEPES buffer (pH 7.4) at 25 °C. Time-resolved emission spectra of **[Tb-5]** were measured every 10 min ($0 \approx 100$ min) after the addition of β-galactosidase.

galactosidase (113 nM) to an aqueous solution of **[Tb-5]** resulted in a decrease in the luminescence of Tb^{3+} as shown in Figure 6c. The luminescence intensity at 545 nm of the **[Tb-5]** solution decreased by about 43 % of the initial luminescence intensity when β-galactosidase was added. HPLC monitoring of the conversion of **[Tb-5]** into **[Tb-8]** confirmed the removal of the galactopyranose residue of **[Tb-5]** with a concomitant luminescence decrease (data not shown). The kinetic parameters for the enzyme reaction of **[Tb-5]** with β-galactosidase were determined by measuring the luminescence change of **[Tb-5]**, because it is well known that the linear relationship of the longitudinal relaxation rates, $1/T_1$, of the water protons is valid only if the concentration of the paramagnetic species, Gd^{3+}, is at the level of mmol or submmol per kilogram of solvent (millimolality or submillimolality),[2] whereas for the determination of the ki-

netic parameters, the β-galactosidase substrate concentration should be in the range of several μM ≈ several hundred μM. Kinetic parameters K_m and k_{cat} were determined by direct fitting of the initial velocity versus substrate concentration data to the Michaelis–Menten equation (see Supporting Information). The values of K_m, k_{cat}, and k_{cat}/K_m of **[Tb-5]** for β-galactosidase were 81.6 μM, 2.7 s^{-1}, and 33.1 $mM^{-1}s^{-1}$, respectively. For reference, the values for *o*-nitrophenyl β-D-galactoside (ONPG) and phenyl β-D-galactoside (PG) for β-galactosidase have been reported to be $K_m = 100$ and 90 μM, $k_{cat} = 600$ and 35 s^{-1}, $k_{cat}/K_m = 6000$ and 389 $mM^{-1}\,s^{-1}$, respectively.[25] The reactivity of **[Tb-5]** for β-galactosidase is likely to be sufficient for the detection of enzyme activity in biological systems, on the basis of the kinetic parameters of ONPG and PG, and the experimental data from refs. [10a,b] and [26]. The k_{cat}/K_m value of **[Tb-5]** is probably determined by the structure of the biphenyl group which is the albumin binding moiety,[27] so it should be possible to modulate the k_{cat}/K_m value of **[Tb-5]** for β-galactosidase by modifying the structure of the albumin binding moiety. Moreover, the reactivity of **[Tb-5]** with β-galactosidase appears to be much higher than that of the β-galactosidase-activated MRI probe which was reported by Meade and co-workers.[10b]

Luminescence and chemical properties of [Tb-5] and [Tb-8]: We further investigated in the luminescence and chemical properties of **[Tb-5]** and **[Tb-8]**, and these properties are summarized in Table 2. The luminescence quantum yields (φ) of **[Tb-5]** and **[Tb-8]** were 0.4 and 0.2%, respectively, under air-equilibrated conditions (Table 2). This result corresponds to the phenomenon of the luminescence intensity decrease of **[Tb-5]** in the presence of β-galactosidase. These luminescence quantum yields are relatively low, as compared with those reported for highly luminescent lanthanide complexes,[23f,g,k] but they are sufficiently large for luminescence detection, as described above. Measurement of the decay rate constants of the Tb^{3+} excited state for **[Tb-5]** and **[Tb-8]** were carried out in both H_2O and D_2O. The luminescence lifetimes of **[Tb-5]** and **[Tb-8]** were found to be 0.77 and 0.23 ms in H_2O (τ_{H_2O}), and 1.03 and 0.43 ms in D_2O (τ_{D_2O}), respectively (Table 2). The luminescence lifetime of **[Tb-8]** which is shorter than that of **[Tb-5]** may cause the difference of luminescence intensity between **[Tb-5]** and **[Tb-8]**. These luminescence lifetimes also indicated that the numbers of coordinated water molecules (q values) at the metal center, Tb^{3+}, were 1.35 and 9.8 for **[Tb-5]** and **[Tb-8]**, respectively (Table 2), according to Equation (7).[29a,b]

Number of water molecules :

$$q^{Tb} = 5(1/\tau_{H_2O} - 1/\tau_{D_2O} - 0.06) \quad (7)$$

The q value of **[Tb-5]** is reasonable, considering the experimental data of longitudinal relaxation time (T_1) and long-lived luminescence measurements in this paper, and indicates that **[Tb-5]** has approximately one water molecule coordinated to the chelated Tb^{3+}. Further, in general, the lanthanide trivalent ion (Ln^{3+}) (such as, Eu^{3+}, Gd^{3+}, Tb^{3+}) complexes of DTPA-monoamide or DTPA-bisamide derivatives, which have a coordination number of eight for Ln^{3+}, have approximately one metal-bound water molecule.[4,21a,23f,30] However, the q value of **[Tb-8]** was extremely large, 9.8, showing inconsistency with other experimental data herein, and therefore this calculated value seems not to reflect the number of water molecules coordinated to the central metal ion, Tb^{3+}. Other factors could account for this extremely large q value of **[Tb-8]**, and the mechanism of this abnormal feature of **[Tb-8]** is now under investigation.

Table 2. Luminescence and chemical properties.

Compound	φ [%][a]	τ_{H_2O} [ms][b]	τ_{D_2O} [ms][c]	q[d]
[Tb-5]	0.4	0.77	1.03	1.35
[Tb-8]	0.2	0.23	0.43	–[e]

[a] Quantum yields were calculated by using quinine sulfate ($\varphi = 0.546$ in 1 N H_2SO_4)[28] as a standard, and measured in 100 mM HEPES buffer; pH 7.4. [b] In H_2O-based buffer (100 mM HEPES buffer, pH 7.4). [c] In D_2O-based buffer (100 mM HEPES buffer, pD 7.4). [d] The q values were estimated by using the equation $q^{Tb} = 5(1/\tau_{H_2O} - 1/\tau_{D_2O} - 0.06)$, which allows for the contribution of unbound water molecules.[29a,b] [e] The chelated q value of **[Tb-8]** was extremely large (9.8), and this value seems not to reflect the number of coordinated water molecules to the centered metal ion, Tb^{3+}. Other factors may account for this extremely large q value.

Conclusion

The Gd^{3+} complex **[Gd-5]** is the first RIME-based β-galactosidase-activated MRI contrast agent, and our design strategy should be applicable to a range of new types of β-galactosidase-activated MRI contrast agents, which may possess novel chemical characteristics, such as, various reactivity with β-galactosidase, specific biodistribution in living specimens and cells, differing extent of r_1 relaxivity change, and so on. This bioactive MRI contrast agent **[Gd-5]** should be useful for studies on the gene expression of lacZ in biological systems.[1a,8,10]

Experimental Section

All reagents were purchased from Tokyo Kasei Kogyo Co. Ltd. (Japan), Wako Pure Chemical Industries Ltd. (Japan), or Aldrich Chemical Co. Inc. (St. Louis, MO), and were used directly without further purification. All solvents were used after distillation. β-Galactosidase [EC 3.2.1.23] Sigma cat G 6008 (Grade VI: From *Escherichia coli*), HSA (human serum albumin, 97–99%) Sigma cat A 9511 (1×crystallized and lyophilized), albumin from rat serum Sigma cat A 6272, BSA (bovine serum albumin) Sigma cat A 7906 (minimum 98% electrophoresis), and albumin from rabbit serum Sigma cat A 0764 (ca. 99% agarose gel electrophoresis) were purchased from Sigma. Dulbecco's phosphate-buffered saline (D-PBS(−)) Sigma cat 14190–136 was purchased from GIBCO, and was used as phosphate-buffered saline (PBS). Silica gel column chromatography was performed by using BW-300, and Chromatorex-ODS (both from Fuji Silysia Chemical Ltd., Japan). Amberlite IR-120 Plus(H) was purchased from ICN Biomedicals, Inc. (USA). Chelex 100 resin (100–200 mesh, sodium form) was purchased from Bio-Rad Laboratories (USA).

Instruments: ^1H and ^{13}C NMR spectra were recorded by using a JEOL JNM-LA300 spectrometer. Mass spectra were measured by using a JEOL-T100LC AccuTOF mass spectrometer (ESI^+ and ESI^-). HPLC

purification was performed on a reversed-phase column, Inertsil Prep-ODS 30 mm × 250 mm (GL Sciences, Inc. (Tokyo, Japan)) fitted on a Jasco PU-1587 system. Measurements of longitudinal water proton relaxation times (T_1) were made by using an NMR analyzer operating at 20 MHz, 0.47 T (Minispec mq20, Bruker). Time-resolved luminescence spectra were recorded by using a Perkin–Elmer LS-55 (Beaconsfield, Buckinghamshire, England). UV/Vis spectra were obtained by using a Shimadzu UV-1650PC (Tokyo, Japan). Normal fluorescence spectra were measured by using a Hitachi F4500 spectrofluorometer (Tokyo, Japan). Aqueous solutions of Tb^{3+} complexes illuminated at 254 nm were photographed by using a Handy UV lamp (Handy UV Lamp, SLUV-4, AS ONE Co., Japan) (see Supporting Information).

Relaxation-time measurements: The longitudinal water proton relaxation times, T_1, of aqueous solutions of the Gd^{3+} complex **[Gd-5]** or **[Gd-8]** were measured in phosphate-buffered saline (PBS, Dulbecco's phosphate-buffered saline, pH 7.4) or PBS with albumin at 20 MHz, 0.47 T (Minispec mq20, Bruker). The values of T_1 were measured from 10 points generated by using the standard inversion-recovery procedure. The r_1 relaxivity [$mM^{-1}\,s^{-1}$] of **[Gd-5]** or **[Gd-8]** was determined from the slope of the plot of $1/T_1$ versus [**[Gd-5]**] or [**[Gd-8]**] (0.25, 0.325, 0.4, and 0.475 mM) in PBS or PBS with 4.5% w/v HSA at 25 °C or 37 °C.

HPLC analysis: The transformation of **[Gd-5]** or **[Tb-5]** to **[Gd-8]** or **[Tb-8]** was monitored by using HPLC analysis. The HPLC analysis for the transformation of **[Gd-5]** to **[Gd-8]** was performed on a reversed-phase column (Inertsil ODS-3 4.6 × 250 mm (GL Sciences); eluent, a 20-min linear gradient, from 0 to 80% solvent B (solvent A, 0.1 M triethylammonium acetate (pH 6.5); solvent B, acetonitrile/H_2O 4:1); flow rate, 1.0 mL min^{-1}; UV 300 nm). The retention times of **[Gd-5]** and **[Gd-8]** under these conditions were 9.1 and 11.5 min, respectively. The HPLC analysis to measure the transformation of **[Tb-5]** to **[Tb-8]** was performed by using a reversed-phase column (Inertsil ODS-3 4.6 × 250 mm (GL Sciences); eluent, a 70-min linear gradient, from 10 to 80% solvent B (solvent A, 0.1 M triethylammonium acetate (pH 6.5); solvent B, acetonitrile/H_2O 4:1); flow rate, 1.0 mL min^{-1}; UV 280 nm). The retention times of **[Tb-5]** and **[Tb-8]** under these conditions were 7.7 and 14.9 min, respectively.

T_1 relaxation time measurements of [Gd-5] with β-galactosidase: The longitudinal relaxation T_1 times were measured for **[Gd-5]** in the presence of β-galactosidase (113 nM) or heat-inactivated β-galactosidase (10 min at 80 °C) at 113 nM, with 4.5% w/v HSA in PBS (pH 7.4), at 20 MHz, 0.47 T, at 37 °C. The concentration of β-galactosidase was calculated based on a monomer of $M_W = 116.3$ kDa.[31] On HPLC analysis of the reaction mixture, only two peaks of **[Gd-5]** and **[Gd-8]** were detected at 300 nm.

Albumin binding study: The T_1 relaxation times of **[Gd-5]** (0.1 mM) or **[Gd-8]** (0.1 mM) were measured in PBS (pH 7.4) with various concentrations of HSA (0, 0.335, 0.67, 1.005, 1.34, 1.675, 2.01, 2.345, 2.68, 3.015, and 3.35 mM). The concentrations of HSA were determined on the basis of 4.5% w/v = ≈0.67 mM.[4,11a]

Comparison of various species of serum albumins: The longitudinal water proton relaxation times T_1 of **[Gd-5]** or **[Gd-8]** were measured at 37 °C in PBS (pH 7.4) in the presence of 4.5% w/v serum albumin from four different species (human, rat, bovine, and rabbit) in the presence or absence of β-galactosidase (1.13 μM).

UV/Vis absorption spectral measurements: The absorption spectra of **[Tb-5]** (50 μM) or **[Tb-8]** (50 μM) were measured at 25 °C in aqueous solution buffered to pH 7.4 (100 mM HEPES buffer).

Time-resolved luminescence spectral measurements: The time-resolved luminescence spectra of **[Tb-5]** or **[Tb-8]** (50 μM, respectively) were measured in 100 mM HEPES buffer at pH 7.4, 25 °C (excitation at 280 nm for **[Tb-5]** and **[Tb-8]**, respectively). The slit width was 10 nm for both excitation and emission. A delay time of 50 μs and a gate time of 1.00 ms were used.

Kinetic studies: Kinetic parameters K_m and k_{cat} were determined by direct fitting of the initial velocity versus substrate (**[Tb-5]**) concentration data to the Michaelis–Menten equation as shown in the Supporting Information. The initial velocities were determined by monitoring the decrease of the Tb^{3+} luminescence of **[Tb-5]** solutions at 37 °C in PBS (pH 7.4) (excitation 280 nm, emission 545 nm) with a Hitachi F4500 spectrofluorometer, in the presence of β-galactosidase (151 nM) and various concentrations of **[Tb-5]** (5, 10, 20, 40, 80, and 160 μM). The slit width was 5 nm for both excitation and emission. The photomultiplier voltage was 700 V.

Quantum yield measurements: The luminescence spectra were measured with a Hitachi F4500 spectrofluorometer. The slit width was 2.5 nm for both excitation and emission. The photomultiplier voltage was 700 V. The luminescence spectra of **[Tb-5]** or **[Tb-8]** were measured in 100 mM HEPES buffer at pH 7.4, 25 °C, with irradiation at 280 nm. The quantum yields of Tb^{3+} complexes were evaluated by using a relative method with reference to a luminescence standard, quinine sulfate ($\varphi = 0.546$ in 1 N H_2SO_4).[28] The quantum yields of Tb^{3+} complexes can be expressed by Equation (9)[32]:

$$\Phi_x/\Phi_{st} = [A_{st}/A_x][n_x^2/n_{st}^2][D_x/D_{st}] \quad (8)$$

where Φ is the quantum yield (subscript "st" stands for the reference and "x" for the sample), A is the absorbance at the excitation wavelength, n is the refractive index, and D is the peak area (on an energy scale) of the luminescence spectra. The samples and the reference were excited at the same wavelength (280 nm). The sample and the reference absorbance at the excitation wavelength were kept as low as possible to avoid fluorescence errors ($A_{exc} < 0.05$).

Luminescence lifetime measurements: The luminescence lifetimes of the Tb^{3+} complexes were recorded on a Perkin–Elmer LS-55 instrument. The data were collected with a 10-μsec resolution in H_2O (100 mM HEPES buffer at pH 7.4) and D_2O (100 mM HEPES buffer at pD 7.4, based on the equation pD = pH + 0.40[33]) at 25 °C, and fitted to a single-exponential curve obeying Equation (9):

$$I = I_0 \exp(-t/\tau) \quad (9)$$

where I_0 and I are the luminescence intensities at the time $t = 0$ and time t, respectively, and τ is the luminescence emission lifetime. Lifetimes were obtained by monitoring the emission intensity at 545 nm (excitation at 280 nm).

Acknowledgement

This work was supported by the Ministry of Education, Culture, Sports, Science and Technology of Japan (Grants for The Advanced and Innovational Research Program in Life Sciences, 16370071 and 16659003 to T.N., 15681012, 17035019, 17036012, 017048006, and 17651119 to K.K.). T.N. was also supported by the Hoh-ansha Foundation. K.K. was also supported by the Sankyo Foundation, by the Kanagawa Academy of Science, and by the Shimadzu Foundation. K.H. was the recipient of Research Fellowships of the Japan Society for the Promotion of Science for Young Scientists. We thank Professor Haruhiko Bito for valuable suggestions.

[1] a) G. Genove, U. DeMarco, H. Xu, W. F. Goins, E. T. Ahrens, *Nat. Med.* **2005**, *11*, 450–454; b) K. H. Thompson, C. Orvig, *Science* **2003**, *300*, 936–939; c) K. Nakahara, T. Hayashi, S. Konishi, Y. Miyashita, *Science* **2002**, *295*, 1532–1536; d) H. Degani, V. Gusis, D. Weinstein, S. Fields, S. Strano, *Nat. Med.* **1997**, *3*, 780–782; e) R. E. Jacobs, S. E. Fraser, *Science* **1994**, *263*, 681–684; f) J. C. Frias, K. J. Williams, E. A. Fisher, Z. A. Fayad, *J. Am. Chem. Soc.* **2004**, *126*, 16316–16317.

[2] A. E. Merbach, É. Tóth, *The Chemistry of Contrast Agents in Medical Magnetic Resonance Imaging*, Wiley, New York, **2001**.

[3] a) S. Aime, M. Botta, M. Fasano, E. Terreno, *Acc. Chem. Res.* **1999**, *32*, 941–949; b) S. Aime, M. Botta, M. Fasano, E. Terreno, *Chem. Soc. Rev.* **1998**, *27*, 19–29.
[4] P. Caravan, J. J. Ellison, T. J. McMurry, R. B. Lauffer, *Chem. Rev.* **1999**, *99*, 2293–2352.
[5] V. M. Runge, D. Y. Gelblum, M. L. Pacetti, F. Carolan, G. Heard, *Radiology* **1990**, *177*, 393–400.
[6] a) M. P. Lowe, *Aust. J. Chem.* **2002**, *55*, 551–556; b) L. Thunus, R. Lejeune, *Coord. Chem. Rev.* **1999**, *184*, 125–155; c) V. Comblin, D. Gilsoul, M. Hermann, V. Humblet, V. Jacques, M. Mesbahi, C. Sauvage, J. F. Desreux, *Coord. Chem. Rev.* **1999**, *185–186*, 451–470; d) M. K. Thompson, B. Misselwitz, L. S. Tso, D. M. J. Doble, H. Schmitt-Willich, K. N. Raymond, *J. Med. Chem.* **2005**, *48*, 3874–3877; e) V. C. Pierre, M. Botta, K. N. Raymond, *J. Am. Chem. Soc.* **2005**, *127*, 504–505; f) H. Kato, Y. Kanazawa, M. Okumura, A. Taninaka, T. Yokawa, H. Shinohara, *J. Am. Chem. Soc.* **2003**, *125*, 4391–4397; g) M. Mikawa, H. Kato, M. Okumura, M. Narazaki, Y. Kanazawa, N. Miwa, H. Shinohara, *Bioconjugate Chem.* **2001**, *12*, 510–514; h) A. Accardo, D. Tesauro, P. Roscigno, E. Gianolio, L. Paduano, G. D'Errico, C. Pedone, G. Morelli, *J. Am. Chem. Soc.* **2004**, *126*, 3097–3107; i) J. Lee, M. J. Zylka, D. J. Anderson, J. E. Burdette, T. K. Woodruff, T. J. Meade, *J. Am. Chem. Soc.* **2005**, *127*, 13164–13166.
[7] a) T. J. Meade, A. K. Taylor, S. R. Bull, *Curr. Opin. Neurobiol.* **2003**, *13*, 597–602; b) J. A. Duimstra, F. J. Femia, T. J. Meade, *J. Am. Chem. Soc.* **2005**, *127*, 12847–12855; c) W. Li, S. E. Fraser, T. J. Meade, *J. Am. Chem. Soc.* **1999**, *121*, 1413–1414; d) W. Li, G. Parigi, M. Fragai, C. Luchinat, T. J. Meade, *Inorg. Chem.* **2002**, *41*, 4018–4024; e) S. Zhang, K. Wu, A. D. Sherry, *Angew. Chem.* **1999**, *111*, 3382–3384; *Angew. Chem. Int. Ed.* **1999**, *38*, 3192–3194; f) N. Raghunand, C. Howison, A. D. Sherry, S. Zhang, R. J. Gillies, *Magn. Reson. Med.* **2003**, *49*, 249–257; g) É. Tóth, R. D. Bolskar, A. Borel, G. González, L. Helm, A. E. Merbach, B. Sitharaman, L. J. Wilson, *J. Am. Chem. Soc.* **2005**, *127*, 799–805; h) M. Mikawa, N. Miwa, M. Bräutigam, T. Akaike, A. Maruyama, *J. Biomed. Mater. Res.* **2000**, *49*, 390–395; i) M. Mikawa, T. Yokawa, N. Miwa, M. Brautigam, T. Akaike, A. Maruyama, *Acad. Radiol.* **2002**, *9*, S109–S111; j) K. E. Løkling, R. Skurtveit, A. Bjørnerud, S. L. Fossheim, *Magn. Reson. Med.* **2004**, *51*, 688–696; k) S. Aime, M. Botta, E. Gianolio, E. Terreno, *Angew. Chem.* **2000**, *112*, 763–766; *Angew. Chem. Int. Ed.* **2000**, *39*, 747–750; l) K. Hanaoka, K. Kikuchi, Y. Urano, M. Narazaki, T. Yokawa, S. Sakamoto, K. Yamaguchi, T. Nagano, *Chem. Biol.* **2002**, *9*, 1027–1032; m) K. Hanaoka, K. Kikuchi, Y. Urano, T. Nagano, *J. Chem. Soc. Perkin Trans. 2* **2001**, 1840–1843; n) R. Trokowski, S. Zhang, A. D. Sherry, *Bioconjugate Chem.* **2004**, *15*, 1431–1440.
[8] a) D. Högemann, J. P. Basilion, *Eur. J. Nucl. Med.* **2002**, *29*, 400–408; b) R. Weissleder, A. Moore, R. Mahmood, R. Bhorade, H. Benveniste, E. A. Chiocca, J. P. Basilion, *Nat. Med.* **2000**, *6*, 351–354.
[9] D. J. Spergel, U. Krüth, D. R. Shimshek, R. Sprengel, P. H. Seeburg, *Prog. Neurobiol.* **2001**, *63*, 673–686.
[10] a) A. Y. Louie, M. M. Hüber, E. T. Ahrens, U. Rothbächer, R. Moats, R. E. Jacobs, S. E. Fraser, T. J. Meade, *Nat. Biotechnol.* **2000**, *18*, 321–325; b) R. A. Moats, S. E. Fraser, T. J. Meade, *Angew. Chem.* **1997**, *109*, 749–752; *Angew. Chem. Int. Ed. Engl.* **1997**, *36*, 726–728; c) M. M. Alauddin, A. Y. Louie, A. Shahinian, T. J. Meade, P. S. Conti, *Nucl. Med. Biol.* **2003**, *30*, 261–265.
[11] a) P. Cravan, N. J. Cloutier, M. T. Greenfield, S. A. McDermid, S. U. Dunham, J. W. M. Bulte, J. C. Amedio, Jr., R. J. Looby, R. M. Supkowski, W. Dew. Horrocks, Jr., T. J. McMurry, R. B. Lauffer, *J. Am. Chem. Soc.* **2002**, *124*, 3152–3162; b) S. Amie, E. Gianolio, E. Terreno, G. B. Giovenzana, R. Pagliarin, M. Sisti, G. Palmisano, M. Botta, M. P. Lowe, D. Parker, *J. Biol. Inorg. Chem.* **2000**, *5*, 488–497; c) S. Aime, M. Botta, S. G. Crich, G. B. Giovenzana, R. Pagliarin, M. Piccinini, M. Sisti, E. Terreno, *J. Biol. Inorg. Chem.* **1997**, *2*, 470–479.
[12] R. B. Lauffer, T. J. McMurry, S. O. Dunham, D. M. Scott, D. J. Parmelee, S. Dumas, PCT Int. Appl. WO 9736619, **1997**.
[13] A. L. Nivorozhkin, A. F. Kolodziej, P. Caravan, M. T. Greenfield, R. B. Lauffer, T. J. McMurry, *Angew. Chem.* **2001**, *113*, 2987–2990; *Angew. Chem. Int. Ed.* **2001**, *40*, 2903–2906.
[14] L. M. De León-Rodríguez, A. Ortiz, A. L. Weiner, S. Zhang, Z. Kovacs, T. Kodadek, A. D. Sherry, *J. Am. Chem. Soc.* **2002**, *124*, 3514–3515.
[15] P. L. Anelli, I. Bertini, M. Fragai, L. Lattuada, C. Luchinat, G. Parigi, *Eur. J. Inorg. Chem.* **2000**, 625–630.
[16] L. Josephson, J. M. Perez, R. Weissleder, *Angew. Chem.* **2001**, *113*, 3304–3306; *Angew. Chem. Int. Ed.* **2001**, *40*, 3204–3206.
[17] J. W. Chen, W. Pham, R. Weissleder, A. Bogdanov, Jr., *Magn. Reson. Med.* **2004**, *52*, 1021–1028.
[18] M. Zhao, L. Josephson, Y. Tang, R. Weissleder, *Angew. Chem.* **2003**, *115*, 1413–1416; *Angew. Chem. Int. Ed.* **2003**, *42*, 1375–1378.
[19] S. Aime, M. Chiaussa, G. Digilio, E. Gianolio, E. Terreno, *J. Biol. Inorg. Chem.* **1999**, *4*, 766–774.
[20] S. Aime, M. Botta, M. Fasano, S. G. Crich, E. Terreno, *J. Biol. Inorg. Chem.* **1996**, *1*, 312–319.
[21] a) D. Parker, J. A. G. Williams, *J. Chem. Soc. Dalton Trans.* **1996**, 3613–3628; b) D. Parker, *Coord. Chem. Rev.* **2000**, *205*, 109–130; c) G. R. Choppin, D. R. Peterman, *Coord. Chem. Rev.* **1998**, *174*, 283–299.
[22] P. R. Selvin, T. M. Rana, J. E. Hearst, *J. Am. Chem. Soc.* **1994**, *116*, 6029–6030.
[23] a) I. Hemmilä, S. Webb, *Drug Discovery Today* **1997**, *2*, 373–381; b) A. J. Kolb, P. V. Kaplita, D. J. Hayes, Y. W. Park, C. Pernell, J. S. Major, G. Mathis, *Drug Discovery Today* **1998**, *3*, 333–342; c) V. Laitala, I. Hemmilä, *Anal. Chem.* **2005**, *77*, 1483–1487; d) J. Karvinen, V. Laitala, M. L. Mäkinen, O. Mulari, J. Tamminen, J. Hermonen, P. Hurskainen, I. Hemmilä, *Anal. Chem.* **2004**, *76*, 1429–1436; e) Y. Koshi, E. Nakata, I. Hamachi, *ChemBioChem* **2005**, *6*, 1349–1352; f) K. Hanaoka, K. Kikuchi, H. Kojima, Y. Urano, T. Nagano, *J. Am. Chem. Soc.* **2004**, *126*, 12470–12476; g) N. Weibel, L. J. Charbonnière, M. Guardigli, A. Roda, R. Ziessel, *J. Am. Chem. Soc.* **2004**, *126*, 4888–4896; h) M. K. Johansson, R. M. Cook, J. Xu, K. N. Raymond, *J. Am. Chem. Soc.* **2004**, *126*, 16451–16455; i) Z. Lin, M. Wu, M. Schäferling, O. S. Wolfbeis, *Angew. Chem.* **2004**, *116*, 1767–1770; *Angew. Chem. Int. Ed.* **2004**, *43*, 1735–1738; j) K. Lee, V. Dzubeck, L. Latshaw, J. P. Schneider, *J. Am. Chem. Soc.* **2004**, *126*, 13616–13617; k) S. Mameri, L. J. Charbonnière, R. F. Ziessel, *Inorg. Chem.* **2004**, *43*, 1819–1821; l) C. Li, G. L. Law, W. T. Wong, *Org. Lett.* **2004**, *6*, 4841–4844; m) J. C. Frias, G. Bobba, M. J. Cann, C. J. Hutchison, D. Parker, *Org. Biomol. Chem.* **2003**, *1*, 905–907; n) K. J. Franz, M. Nitz, B. Imperiali, *ChemBioChem* **2003**, *4*, 265–271; o) J. P. Cross, M. Lauz, P. D. Badger, S. Petoud, *J. Am. Chem. Soc.* **2004**, *126*, 16278–16279.
[24] D. Parker, R. S. Dickins, H. Puschmann, C. Crossland, J. A. K. Howard, *Chem. Rev.* **2002**, *102*, 1977–2010.
[25] O. Viratelle, J. P. Tenu, J. Garnier, J. Yon, *Biochem. Biophys. Res. Commun.* **1969**, *37*, 1036–1041.
[26] a) Y. Urano, M. Kamiya, K. Kanda, T. Ueno, K. Hirose, T. Nagano, *J. Am. Chem. Soc.* **2005**, *127*, 4888–4894; b) J. Hofmann, M. Sernetz, *Anal. Biochem.* **1983**, *131*, 180–186.
[27] J. P. Tenu, O. M. Viratelle, J. Garnier, J. Yon, *Eur. J. Biochem.* **1971**, *20*, 363–370.
[28] W. H. Helhuish, *J. Phys. Chem.* **1961**, *65*, 229–235.
[29] a) A. Beeby, I. M. Clarkson, R. S. Dickins, S. Faulkner, D. Parker, L. Royle, A. S. de Sousa, J. A. G. Williams, M. Woods, *J. Chem. Soc. Perkin Trans. 2* **1999**, 493–503; b) S. Quici, G. Marzanni, M. Cavazzini, P. L. Anelli, M. Botta, E. Gianolio, G. Accorsi, N. Armaroli, F. Barigelletti, *Inorg. Chem.* **2002**, *41*, 2777–2784.
[30] M. Li, P. R. Selvin, *J. Am. Chem. Soc.* **1995**, *117*, 8132–8138.
[31] A. V. Fowler, I. Zabin, *J. Biol. Chem.* **1978**, *253*, 5521–5525.
[32] Q. Y. Chen, C. J. Feng, Q. H. Luo, C. Y. Duan, X. S. Yu, D. J. Liu, *Eur. J. Inorg. Chem.* **2001**, 1063–1069.
[33] Y. M. Wang, Y. J. Wang, Y. L. Wu, *Polyhedron* **1999**, *18*, 109–117.

Received: May 24, 2007
Published online: November 8, 2007

